

Scaling of the frequencies of the type one edge localized modes and their effect on tungsten in JET ITER-like wall discharges.

P. Devynck¹, N. Fedorczak¹, O. Meyer¹ and JET Contributors*

EUROfusion Consortium, JET, Culham Science Centre, Abingdon, OX14 3DB, UK

¹ CEA, IRFM, F-13108 St. Paul-lez-Durance cedex, France

1) Introduction

A database of 250 pulses taken randomly during the experimental campaigns of JET with the ITER-Like wall (ILW) is used to study the frequency dependences of the type I Edge Localized Modes (ELM) [1]. In the database, the average plasma density goes from 3.8 to $10.1 \cdot 10^{19} \text{ m}^{-3}$. The additional heating spans from 5 to 26 MW with Neutral Beam Injection Power (NBI) spanning from 4.8 to 26 MW. The Ion cyclotron resonant frequency heating power (ICRF) is varied from 0 to 4.8 MW. The plasma current is from 1.3 to 3 MA and the Toroidal magnetic field from 1.3 to 2.87 T. The outer strike point position changes from the centre of the horizontal target up to the corner of the vertical one. The signal used to track the dynamics of the ELMs is the tungsten WI neutral spectroscopic line that integrates 10 lines of sight covering the outer divertor. The signals from these lines of sight are filtered with a filter centred on 401 nm and a bandwidth of about 1 nm. A program based on histogram methods and Boolean filtering was developed to select the ELMs out of the WI signal.

2) Scaling of the ELM frequency and interpretation

The best fit of the ELM frequency that was found only include two parameters, the density height of the pedestal N_{ped} and the time averaged maximum drop of pedestal density during ELM crash dN_{ped} (figure 1). The exponents of the fit are 0.99 for N_{ped} and -1.08 for dN_{ped} . The standard deviation of the data around the fit is 10 Hz. It is clear that the data are compatible with a simple relationship such as $f_{\text{ELM}} \propto N_{\text{ped}} / dN_{\text{ped}}$. This fit is different from the one that is usually found in Carbon components machines where the power through the separatrix and the plasma current is found to drive the ELM frequency.

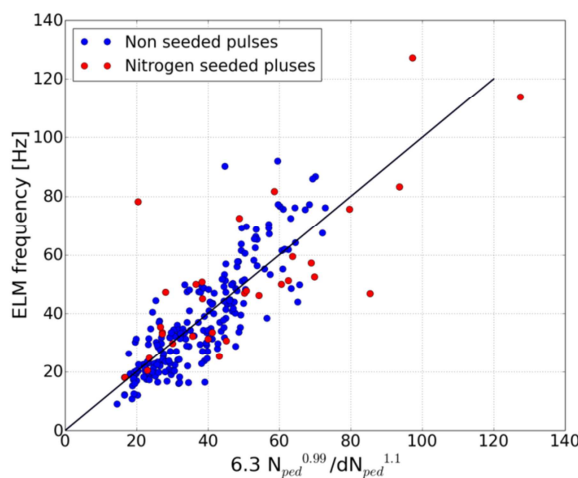


Figure 1
best fit found
for the ELM
frequency
with N_{ped} and
 dN_{ped} .

*See the author list of "Overview of the JET results in support to ITER" by X. Litaudon et al. accepted for publication in Nuclear Fusion Special issue: overview and summary reports from the 26th Fusion Energy Conference (Kyoto, Japan, 17-22 October 2016)

The dependence of the ELM period on dN_{ped} suggests that it is the time needed to reconstruct the pedestal density that is the driving term. We assume that the refill of the pedestal density is governed by particles coming from the external regions of the plasma. It is conjectured that it occurs with the help of neutrals crossing the separatrix and which are then ionized in the pedestal region. In order to describe this, we are going to use a simplified 1 D model in slab geometry and assume that the dynamics occurs only in the radial direction. We write first the equation for the variation of the density in the pedestal region just after the ELM crash.

$$\frac{\partial n_e}{\partial t} + \nabla \Gamma_e = n_e n_o \langle \sigma_{iz} v_e \rangle \quad (1)$$

Where Γ_e is the outward particle flux and the right hand side is the source term that comes from the ionization of the neutrals n_o in the pedestal region. We assume that the radial flux in the pedestal that is known to be turbulent can be described with a diffusion coefficient D_{\perp} that we keep constant in the pedestal region: $\Gamma_e = D_{\perp} \nabla n_e$. To simplify further, we use here an exponential function for the density profile that can be easily linearized:

$$n_e(x) = n_{eo} e^{-x/\Delta_{ped}}$$

Where n_{eo} is the density at the radial position of the top of the pedestal, and Δ_{ped} is the width of the pedestal. With these hypotheses the term $\nabla \Gamma_e$ can be evaluated and gives $D_{\perp} n_e / (\Delta_{ped})^2$. Relation 1 can be rewritten as:

$$\frac{\partial n_e}{\partial t} = n_e n_o \langle \sigma_{iz} v_e \rangle - \frac{D_{\perp}}{\Delta_{ped}^2} n_e$$

This relation can be integrated and gives:

$$[\log(n_e)]_{N_{ped}-dN_{ped}}^{N_{ped}} = \int_0^{\tau_E} (n_o \langle \sigma_{iz} v_e \rangle - \frac{D_{\perp}}{\Delta_{ped}^2}) dt \quad (2)$$

Here N_{ped} is the density of the pedestal before the ELM crash, dN_{ped} is the total density drop of the pedestal after the crash and τ_E is the time needed to refill the density of the pedestal. We take the inverse of this time to be the ELM frequency. We simplify the problem by taking a time averaged value for the expression in between the brackets in the integral. We also take $dN_{ped}/N_{ped} < 1$ so that the logarithm on the left hand side of relation 2 can be simplified. With all these simplifications relation 2 becomes:

$$\frac{dN_{ped}}{N_{ped}} \approx \langle n_o \langle \sigma_{iz} v_e \rangle - \frac{D_{\perp}}{\Delta_{ped}^2} \rangle \tau_E$$

And finally $f_E \approx \langle n_o \langle \sigma_{iz} v_e \rangle - \frac{D_{\perp}}{\Delta_{ped}^2} \rangle \frac{N_{ped}}{dN_{ped}}$ (3)

3) Temperature versus density for pedestal pressure recovery time.

We find that in the case of JET, the temperature of the pedestal apparently does not play a role in setting the ELM frequency. Although in all these pulses an effect of the ELMs on the temperature pedestal is also found. In order to understand this, we plot in Figure 2 the

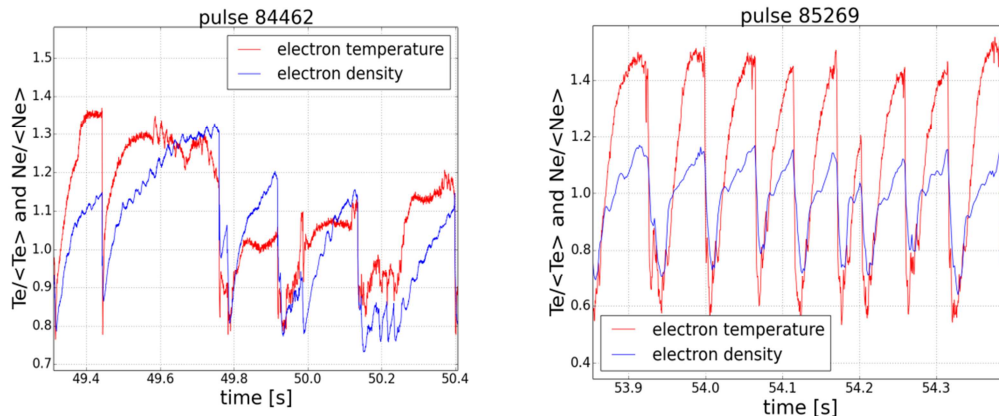


Figure 2

Time traces of density and temperature in the pedestal. Left: Pulse 84462, 11.5 MW NBI Heating, no gas fuelling. Right: Pulse 85269, 16 MW NBI heating, 4 MW ICRH, with gas fueling.

behaviour of both temperature and density as a function of time. The data for the temperature is the sum of 6 ECE channels on the low field side scanning radially the pedestal region. The data for density is obtained from an interferometer vertical chord passing through the top of the pedestal. For the no gas injection case, the recovery of the pedestal temperature after the ELM crash occurs before the one of the density. For the high power case (Right), both temperature and density rise until the next ELM is triggered. Notice however that some signs of saturation can be seen on the temperature signal. This figure shows that in any case, the time to reconstruct the pedestal density in JET is longer or equal to the time to rebuild the temperature of the pedestal. This explains that the frequency of the ELMs is set by the recovery time of the density pedestal in JET.

4) Dependences of the amount of tungsten in the discharge

The amount of tungsten in the bulk of the discharge is roughly estimated with the help of the bulk radiated power and mean density of the plasma. This supposes that the radiation from the bulk comes only from tungsten. In this case the relative invariance of the radiative function of tungsten with electron temperature allows writing the amount of tungsten in the discharge as: $\iiint N_w dV = P_{\text{rad,bulk}} / (\langle N_e \rangle L_w^{\text{eff}})$, where L_w^{eff} is taken as a constant. The ratio of Number of tungsten atoms estimated in this way (W_{content}) over tungsten source (W_{source}) during ELMs (estimated with the WI signal) is plotted in Figure 3 as a function of ELM frequency. In this figure, the data are plotted according to the gas puffing level. One notes that the ratio $W_{\text{content}}/W_{\text{source}}$ is a decreasing function of the ELM frequency, indicating that the flushing effect of tungsten by the ELMs is real. This can be observed at all frequencies with a gas puffing larger

than 10^{22} p/s. At low frequencies, the data show a large scatter that occurs at low gas puffing level. In particular, the ratio $W_{\text{content}}/W_{\text{source}}$ is the highest when the gas puffing is smaller 10^{22} p/s. This suggests that the gas injection has some effect on the accumulation of tungsten in the discharge that is maximum at ELM frequency around 20 Hz and lower.

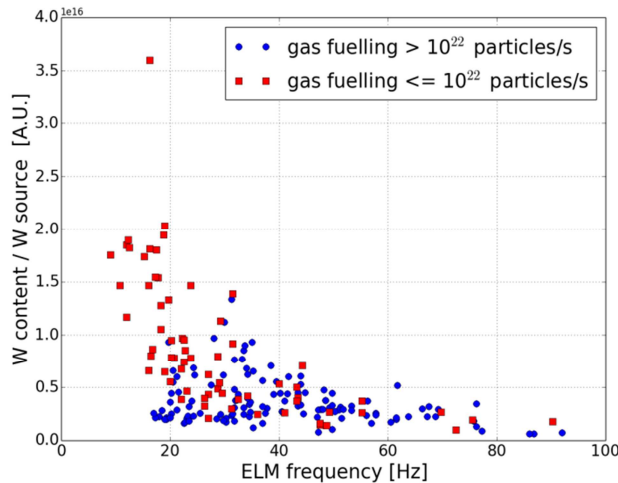


Figure 3

Ratio of W_{content} over W_{source} . The ratio is shown as a function of ELM frequency.

5) Conclusions

This work is dedicated to the analysis of the type I ELM frequency behavior in the JET ILW with the help of a large database. We do not discuss the type of instability triggering the ELMs which is a very important topic that is intensively studied. We put more emphasis on the role played by the neutrals issued from the recycling and the fueling in setting the frequency. The experimental fit of the type I ELM frequency in JET is found to be compatible with a model where the frequency is set by the time needed for the neutrals to reconstruct the density pedestal after the crash [1]. The temperature does not play a role as it is found to recover more rapidly or at the same rate (with the highest level of additional heating and fueling) than the density. Experimentally a dependence of f_{ELM} with P_{sep} (power through separatrix) has been found for some fixed plasma conditions (density and gas injection) in JET ILW [2]. This indicates that P_{sep} probably has an effect on the amplitude of the crash dN_{ped} . We will investigate this in the future. Finally, a flushing effect of tungsten by ELMs is observed. The $W_{\text{content}}/W_{\text{source}}$ curve decreases with ELM frequency but a large scatter exists at low frequencies. The apparent scatter of the data at low ELM frequencies is in fact correlated to the gas injection level. The ratio $W_{\text{content}}/W_{\text{source}}$ is seen to decrease with gas injection level at fixed frequency indicating an additional role of the gas injection to prevent the accumulation of tungsten in the discharge at low ELM frequency [3].

[1] Devynck P. et al. Plasma Phys. Control. Fusion **58** (2016) 125014 (9pp)

[2] Maggi C. F. et al. Nucl. Fusion **55** (2015) 113031 (15pp)

[3] Solano E. R. et al, [Paper P1.006](#) of 41st EPS Conference on Plasma Physics, 2014.

This work has been carried out within the framework of the EUROfusion Consortium and has received funding from the Euratom research and training programme 2014-2018 under grant agreement No 633053. The views and opinions expressed herein do not necessarily reflect those of the European Commission.